

*Current-interchange Instability in a Tubular Layer of an Electron-hole Plasma*

V. V. VLADIMIROV, L. V. DUBOVOI, A. A. KONDAKOV, V. F. SHANSKIĬ, AND A. I. SHCHEDRIN

D. V. Efremov Institute of Electrophysical Apparatus

Submitted August 18, 1971

Zh. Eksp. Teor. Fiz. 62, 578-583 (February, 1972)

Results are presented of an theoretical and experimental study of the conditions for Kadomtsev-Nedospasov current-convective instability arising in hollow cylindrical germanium samples. It is shown that with increasing ratio of the inside and outside radii of the cylinder, the electric and magnetic field threshold values, which are just sufficient for plasma instability to set in, always increase. The presence of an external azimuthal magnetic field may exert a stabilizing effect on the type of instability considered. The results of the theoretical calculations are in satisfactory agreement with the results of the measurements.

**I**N recent years there has been considerable increased interest in the study of the vibrational properties of an electron-hole plasma of a semiconductor. The present study is a continuation of a series of investigations<sup>[1,2]</sup> devoted to a clarification of the main laws governing the excitation of the Kadomtsev-Nedospasov current-convective instability in an electron-hole plasma, and to the development of methods of its stabilization. We have made a theoretical and experimental study of the conditions under which the type of excitation under consideration is excited in germanium samples in the form of hollow cylinders. We investigated the stabilizing influence of an external azimuthal magnetic field  $H_\phi$  on the threshold values of the electric field  $E_z$  and magnetic field  $H_z$ , starting with which the instability sets in. The calculations were performed for the case of an equilibrium and injected electron-hole plasma.

A schematic diagram of the investigated system, the spatial orientation of the field, and the coordinate notation used in the calculations are shown in Fig. 1. Here  $R$  is the outside radius of the cylinder,  $\rho$  the inside radius,  $r$  the running coordinate,  $E_z$  the electric field in the plasma, and  $H_z$  the external longitudinal magnetic field. The auxiliary azimuthal magnetic field  $H_\phi = 2I/cr$  was produced by passing current  $I$  through a copper conductor located in the cavity of the cylinder along its axis.

In the analysis of the stationary state and of the stability of the electron-hole plasma, the initial equations are conveniently written in the form

$$\begin{aligned} v_c &= -\frac{D_e}{n} \nabla n - \frac{b_e}{c} [v_c \mathbf{H}] + b_e \nabla \varphi, \\ v_h &= -\frac{D_h}{n} \nabla n + \frac{b_h}{c} [v_h \mathbf{H}] - b_h \nabla \varphi, \\ \frac{\partial n}{\partial t} + \text{div } n v_e &= Z n, \quad \frac{\partial n}{\partial t} + \text{div } n v_h = Z n, \end{aligned} \tag{1}^*$$

where  $v_{i=e,h}$  are respectively the drift velocities of the electrons and holes;  $D_i$  and  $b_i$  are the diffusion and mobility coefficients,  $Z$  is the coefficient of volume generation of non-equilibrium carriers,  $n$  is the density of the particles,  $\varphi$  is the potential ( $\mathbf{E} = -\nabla\varphi$ ), and  $\mathbf{H}(0, H_\phi, H_z)$  is the magnetic field.

The calculations were carried out in the approxima-

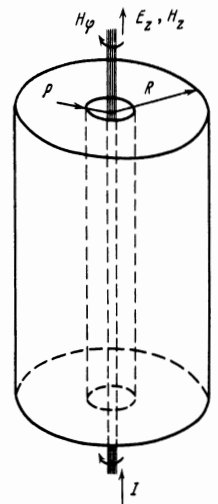


FIG. 1. Spatial orientation of fields and coordinate system used in the paper.

tion  $H_b \mu c \ll 1$  for two cases: a) equilibrium plasma ( $Z = 0$ ) and low velocity of the surface recombination  $S, S \ll D_a / (R - \rho)$ , where  $D_a = (b_e D_h + b_h D_e) / (b_e + b_h)$  is the coefficient of ambipolar diffusion; b) injected plasma ( $Z \neq 0$ ) and large  $S$  corresponding to the inequality  $S \gg D_a / (R - \rho)$ .

Let us consider the equilibrium state of an electron-hole plasma in the presence of an external axial current  $I$ , assuming that all the quantities depend only on the radius.

When  $I \neq 0$ , owing to the transverse magnetic-concentration effect<sup>[3]</sup>, the spatial distribution of the carriers over the cross section has the following form: in case a)

$$n_0 = \alpha r^{-\kappa}, \quad \kappa = 2IE_z b_e b_h / c^2 D_a, \tag{2}$$

where  $\alpha$  is a constant determined from the condition that the number of particles is conserved in the magnetic concentration effect (the criterion for the excitation of the instability is independent of  $\alpha$  in this case, and we do not present the corresponding expression); in case b)

$$n_0 = N_0 r^{-\kappa/2} [J_0(\beta_0 r) + B Y_0(\beta_0 r)] \tag{3}$$

where  $J_0$  and  $Y_0$  are Bessel functions of zero order and of the first and second kind.

Expression (3) has been derived in the approxima-

\* $[v_c \mathbf{H}] \equiv v_c \times \mathbf{H}$ .

tion  $\kappa^2 \ll 1$ . The constants B and  $\beta_0$  are determined from the condition  $n_0(R) = n_0(\rho) = 0$ , as was done in<sup>[4]</sup>, in which a hollow positive gas-discharge column was investigated.

In the analysis of the instability we linearize Eqs. (1) with respect to small perturbations of the type  $A' = A_1(r) \exp(i\omega t - im\varphi - ikz)$ . The equations for the perturbed potential and perturbed density then take the form

$$\begin{aligned} & b_e n_0 \Delta \varphi' + b_e \frac{dn_0}{dr} \frac{d\varphi_1}{dr} + i \frac{b_e^2}{c} H \frac{1}{r} \frac{dn_0}{dr} \varphi_1 - D_e \Delta n_1' + b_e \frac{D_e - D_h}{b_e + b_h} \\ & \times \frac{1}{r} \frac{d}{dr} \left( \frac{rn_1}{n_0} \frac{dn_0}{dr} \right) - \frac{D_e \kappa}{r} \frac{dn_1}{dr} - i \frac{b_e^2}{c} \frac{D_e - D_h}{b_e + b_h} H \frac{1}{rn_0} \frac{dn_0}{dr} n_1 \\ & + (i\omega + ikb_e E_z - Z) n_1 = 0, \\ & b_h n_0 \Delta \varphi' + b_h \frac{dn_0}{dr} \frac{d\varphi_1}{dr} - i \frac{b_h^2}{c} H \frac{1}{r} \frac{dn_0}{dr} \varphi_1 + D_h \Delta n_1' + b_h \frac{D_e - D_h}{b_e + b_h} \\ & \times \frac{1}{r} \frac{d}{dr} \left( \frac{rn_1}{n_0} \frac{dn_0}{dr} \right) + \frac{D_e \kappa}{r} \frac{dn_1}{dr} + i \frac{b_h^2}{c} \frac{D_e - D_h}{b_e + b_h} H \frac{1}{rn_0} n_1 \\ & - (i\omega - ikb_h E_z - Z) n_1 = 0, \end{aligned} \quad (4)$$

where  $H = (mH_Z - 2kI/c)$ .

Equating the instability-induced radial flux of the electrons and holes to the number of particles that vanish as a result of recombination on the walls, we obtain the boundary conditions:

$$\begin{aligned} & b_e n_0 \frac{d\varphi_1}{dr} + i \frac{b_e^2}{c} H \frac{n_0}{r} \varphi_1 - D_e \frac{dn_1}{dr} + \left( \frac{D_e}{n_0} \frac{dn_0}{dr} - i \frac{b_e}{c} \frac{D_e H}{r} - S \right) n_1 \Big|_{r=R, \rho} = 0, \\ & b_h n_0 \frac{d\varphi_1}{dr} - i \frac{b_h^2}{c} H \frac{n_0}{r} \varphi_1 + D_h \frac{dn_1}{dr} - \left( \frac{D_h}{n_0} \frac{dn_0}{dr} + i \frac{b_h}{c} \frac{D_h H}{r} - S \right) n_1 \Big|_{r=R, \rho} = 0. \end{aligned} \quad (5)$$

In case (a), the solution of Eqs. (4) at  $\kappa^2 \ll 1$  has been obtained by perturbation theory, with  $n_1$  and  $\varphi_1$  represented in the form

$$n_1 = n_{10} + \kappa n_{11}, \quad \varphi_1 = \varphi_{10} + \kappa \varphi_{11}. \quad (6)$$

The expression for  $n_{10}$  and  $\varphi_{10}$  are ( $m^2 = 1$ )

$$\begin{aligned} & n_{10} = r^{-\kappa/2} [C_1 I_1(\beta r) + C_2 K_1(\beta r)], \\ & \varphi_{10} = r^{-\kappa/2} \{ A [C_1 I_1(\beta r) + C_2 K_1(\beta r)] + C_3 I_1(kr) + C_4 K_1(kr) \}, \end{aligned} \quad (7)$$

where

$$A = \frac{1}{\alpha} \left( \frac{D_e - D_h}{b_e + b_h} - \frac{kED_a}{\omega} \right), \quad \beta^2 = k^2 + \frac{i\omega}{D_a};$$

$I_1$  and  $K_1$  are Bessel functions of first order and imaginary argument. When  $\kappa = 0$ , Eqs. (7) coincide with the corresponding expressions of<sup>[5]</sup>. We do not present the expressions for  $n_{11}$  and  $\varphi_{11}$ , since they are too cumbersome. Substituting the solutions (6) in the boundary conditions (5) at  $S = 0$ , we obtained a dispersion relation which we investigated by numerical methods.

Figure 2 shows the dependence of the quantity  $\beta = -b_e b_h R m E_Z H_Z / c D_a$  near the threshold of the oscillator excitation ( $|m| = 1$ ) on  $R/\rho$  at  $\kappa = 0$  (current  $I = 0$ ). As seen from this figure (curve 1), the excitation threshold increases with decreasing tube wall thickness, owing to the increasing role of the diffusion.

Figure 3 shows the dependence of  $\beta$  on  $\kappa$  (curve 1) at  $\rho/R = 0.5$  (the corresponding plots at other values of  $\rho/R$  are similar). At small values of  $\kappa$ , when  $\kappa > 0$  (the current  $I$  has the same direction as the current in the sample), it is easier to excite the instability in the semiconductor, since the additional drift flux  $\alpha \kappa$

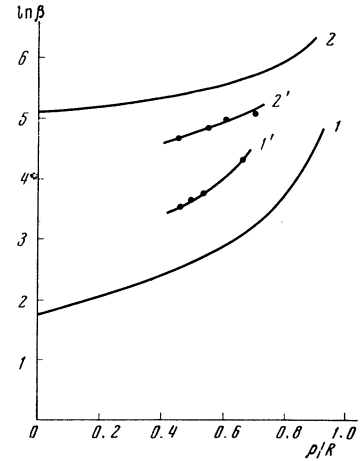


FIG. 2. Dependence of the oscillistor excitation threshold on the ratio of the internal radius of the cylinder to the external one (curves 1 and 2—calculated; 1' and 2'—experimental; 1' corresponds to  $S_1$  and 2' to  $S_2$ ;  $S_1 < S_2$ ).

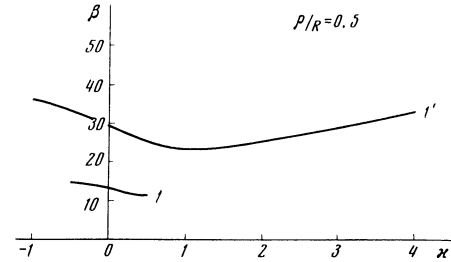


FIG. 3. Dependence of the oscillistor excitation threshold on the axial current (1—calculated, 1'—experimental).

due to the azimuthal magnetic field has in this case the same direction as the radial drift flux that causes the instability at  $\kappa = 0$ .

At  $\kappa \gg 1$ , the instability was investigated by the method of profiling  $n_1$  and  $\varphi_1$ . The values of  $n_1$  and  $\varphi_1$  in case (a) were chosen in the form  $n_1, \varphi_1 \sim r^{-\kappa-1} \sim \nabla n_0$ , since the instability is of the drift type.

Equations (4) were multiplied by  $n_1(\varphi_1)$  and integrated over the tube cross section. The excitation criterion takes in this case the form

$$\begin{aligned} & |\beta| > 2\kappa^2 R / \rho, \quad \rho \neq 0; \quad \text{for } \kappa > 0 \\ & |\beta| > 2\kappa^2. \quad \text{for } \kappa < 0 \end{aligned} \quad (8)$$

Thus, at large values of the current  $I$ , the criterion for the oscillistor excitation becomes more stringent regardless of its direction, owing to the decisive role of the diffusion fluxes.

In case (b), the dependence of the oscillistor excitation threshold on  $\rho/R$  was calculated by the methods used in<sup>[4]</sup> (Fig. 2, curve 2).

The experimental investigation was carried out on electron-hole plasma injected from contacts into hollow cylindrical germanium samples. The samples of length  $L = 10$  cm and different ratios  $\rho/R$  were prepared of single-crystal Ge ( $\rho = 45$  ohm-cm at  $T = 300^\circ\text{K}$ ) with the aid of ultrasound and were etched, after fusing-in the contacts, in CP-4 solution to decrease the rate of surface recombination.

In the experiments, the intensity  $H_Z$  of the external

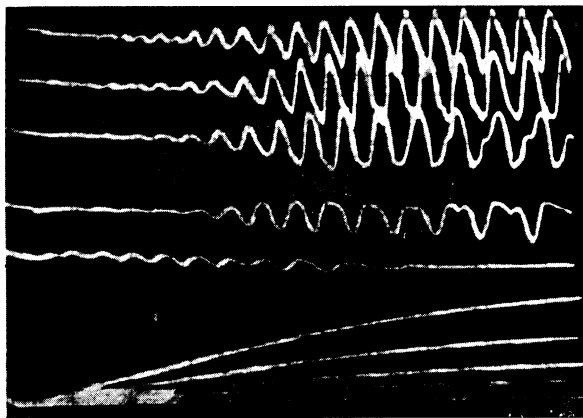


FIG. 4. Oscillograms of current oscillations in the sample circuit (family of five curves in the upper part of the figure), corresponding to different values of the axial current  $I$  (family of five curves in the lower part of the figure).

magnetic field was varied up to 10 kOe; the maximum value of the current  $I$  flowing through the wire inside the sample reached  $I_{\max} = 10^3$  A, and its duration was  $T = 3$  msec. The voltage pulse producing the electric field  $E_z$ , of duration 200  $\mu$ sec, was turned on at the instant when the current through the wire was at a maximum, so that during the measurements the azimuthal magnetic field  $H_\varphi$  could be regarded as constant in time.

To illustrate the effect of the field  $H_\varphi$  on the development of the instability in the plasma, Fig. 4 shows oscillograms of the current oscillations in the sample circuit as functions of the current amplitude  $I$ . At small values of the current  $I$ , the amplitude of the oscillations increases, and then decreases with increasing current  $I$ , vanishing at a certain current value that depends on  $E_z$  and  $H_z$ . The threshold fields

$E_z$  and  $H_z$  at which the instability sets in were determined by the appearance of current oscillations in the sample connected in series with a small resistor.

The experimental plots of the critical fields against  $\rho/R$  and against the value of the axial current  $I$  are shown in Figs. 2 (curves 1' and 2') and 3 (curve 1'). From a comparison of the corresponding curves we see that the results of the theoretical calculations are in satisfactory agreement with the experimental data, thus offering evidence in favor of the correctness of the model chosen in the calculations.

Similar investigations can be of interest in the simulation of phenomena that occur in plasma installations with a turbulent skin layer<sup>[6]</sup>, and also in magnetic traps of the Triax and Levitron type<sup>[7]</sup>. In view of the close analogy between the development of the Kadomtsev-Nedospasov instability in semiconductor and gas-discharge plasmas, it is of interest to study analogous effects in an electron-ion plasma<sup>[8]</sup>.

<sup>1</sup>L. V. Dubovoi and V. F. Shanskii, Zh. Eksp. Teor. Fiz. **56**, 766 (1969) [Sov. Phys. JETP **29**, 416 (1969)].

<sup>2</sup>V. V. Vladimirov, L. V. Dubovoi, and V. F. Shanskii, Zh. Eksp. Teor. Fiz. **58**, 1580 (1970) [Sov. Phys. JETP **31**, 846 (1970)].

<sup>3</sup>H. Suhl and W. Shockley, Phys. Rev. **75**, 1617 (1949).

<sup>4</sup>L. E. Belousova, Zh. Tekh. Fiz. **36**, 892 (1966) [Sov. Phys. Tech. Phys. **11**, 658 (1966)].

<sup>5</sup>C. E. Hurwitz and Mc. Whorter, Phys. Rev. A (1964-1965) **134**, 1033 (1964).

<sup>6</sup>Yu. G. Kalinin, D. N. Lin, L. I. Rudakov, V. D. Ryutov, and V. A. Skoryupin, Zh. Eksp. Teor. Fiz. **59**, 1056 (1970) [Sov. Phys. JETP **32**, 573 (1971)].

<sup>7</sup>L. A. Artsimovich, Upravlyaemye termoyadernye reaktzii (Controlled Thermonuclear Reactions), Fizmatgiz, 1963.

<sup>8</sup>G. V. Gierke and K. H. Wöhler, Nucl. Fusion **1**, 47 (1962)